REPORT DOCUMENTATION PAGE

Form Approved

OMB No. 0704-0188

PLEASE DO NOT RETURN YOUR FORM TO THE ABOVE ADDRESS.

1. REPORT DATE *(DD-MM-YYYY)*	2. REPORT TYPE	3. DATES COVERED *(From - To)*
10-06-2015	Final	20 Mar 13 – 19 Mar 15

4. TITLE AND SUBTITLE

Development of single-molecule DNA sequencing platform based on single-molecule electrical conductance

5a. CONTRACT NUMBER

FA2386-13-1-4035

5b. GRANT NUMBER

Grant AOARD-134035

5c. PROGRAM ELEMENT NUMBER

61102F

6. AUTHOR(S)

Prof. Guewha (Steven) Huang

5d. PROJECT NUMBER

5e. TASK NUMBER

5f. WORK UNIT NUMBER

7. PERFORMING ORGANIZATION NAME(S) AND ADDRESS(ES)

National Chiao Tung University
1001 University Rd EA201A
Hsinchu 300
Taiwan

8. PERFORMING ORGANIZATION REPORT NUMBER

N/A

9. SPONSORING/MONITORING AGENCY NAME(S) AND ADDRESS(ES)

AOARD
UNIT 45002
APO AP 96338-5002

10. SPONSOR/MONITOR'S ACRONYM(S)

AFRL/AFOSR/IOA(AOARD)

11. SPONSOR/MONITOR'S REPORT NUMBER(S)

AOARD-134035

12. DISTRIBUTION/AVAILABILITY STATEMENT

Distribution Code A: Approved for public release, distribution is unlimited.

13. SUPPLEMENTARY NOTES

14. ABSTRACT

The significant findings in this report come from the in vitro, ex vivo, and in vivo evidence data which suggests that gold nanoparticles (GNPs) activate B-cells and enhance immunoglobulin G secretion. GNP treatment upregulates blimp1, downregulates pax5, and enhances downstream IgG secretion. The enhancement is size dependent and time dependent. GNPs ranging from 2 to 12 nm had the maximum stimulatory activity for the production of antibody. This is the first time that specific signal transduction pathway has been unambiguously identified and assigned to nanoparticles in a size-dependent manner. We have thus established the link between physical dimension and biological response at molecular level. In the future, it is possible to imitate this physical stimulation through “non-physical” manipulation, such as genetic control. In particular, the interaction of immune system and nanoparticles could be manipulated through genetic control. The instant advantage is to establish stable and high affinity bionano interface in the fabrication of the unique molecular electronic device, the protein transistor.
New research questions which this research has raised include, how does the immune system sense the size of nanoparticles? Are there size-specific genes?

15. SUBJECT TERMS

Biochemistry, Nanobiotechnology

16. SECURITY CLASSIFICATION OF:			17. LIMITATION OF ABSTRACT	18. NUMBER OF PAGES	19a. NAME OF RESPONSIBLE PERSON
a. REPORT	b. ABSTRACT	c. THIS PAGE			Kristopher, Ahlers, Lt Col, USAF, Ph.D.
U	U	U	SAR	24	19b. TELEPHONE NUMBER *(Include area code)* +81-42-511-2000

Report Documentation Page

Form Approved
OMB No. 0704-0188

1. REPORT DATE	2. REPORT TYPE	3. DATES COVERED
10 JUN 2015	**Final**	**20-03-2013 to 19-03-2015**

4. TITLE AND SUBTITLE **Development of single-molecule DNA sequencing platform**	5a. CONTRACT NUMBER **FA2386-13-1-4035**
	5b. GRANT NUMBER
	5c. PROGRAM ELEMENT NUMBER **61102F**
6. AUTHOR(S) **Guewha(Steven) Huang**	5d. PROJECT NUMBER
	5e. TASK NUMBER
	5f. WORK UNIT NUMBER
7. PERFORMING ORGANIZATION NAME(S) AND ADDRESS(ES) **National Chiao Tung University,1001 University Rd EA201A,Hsinchu 300,Taiwan,NA,NA**	8. PERFORMING ORGANIZATION REPORT NUMBER **N/A**
9. SPONSORING/MONITORING AGENCY NAME(S) AND ADDRESS(ES) **AOARD, UNIT 45002, APO, AP, 96338-5002**	10. SPONSOR/MONITOR'S ACRONYM(S) **AFRL/AFOSR/IOA(AOARD)**
	11. SPONSOR/MONITOR'S REPORT NUMBER(S) **AOARD-134035**

12. DISTRIBUTION/AVAILABILITY STATEMENT
Approved for public release; distribution unlimited

13. SUPPLEMENTARY NOTES

14. ABSTRACT

The significant findings in this report come from the in vitro, ex vivo, and in vivo evidence data which suggests that gold nanoparticles (GNPs) activate B-cells and enhance immunoglobulin G secretion. GNP treatment upregulates blimp1, downregulates pax5, and enhances downstream IgG secretion. The enhancement is size dependent and time dependent. GNPs ranging from 2 to 12 nm had the maximum stimulatory activity for the production of antibody. This is the first time that specific signal transduction pathway has been unambiguously identified and assigned to nanoparticles in a size-dependent manner. We have thus established the link between physical dimension and biological response at molecular level. In the future, it is possible to imitate this physical stimulation through ???nonphysical??? manipulation, such as genetic control. In particular, the interaction of immune system and nanoparticles could be manipulated through genetic control. The instant advantage is to establish stable and high affinity bionano interface in the fabrication of the unique molecular electronic device, the protein transistor. New research questions which this research has raised include, how does the immune system sense the size of nanoparticles? Are there size-specific genes?

15. SUBJECT TERMS
Biochemistry, Nanobiotechnology

16. SECURITY CLASSIFICATION OF:			17. LIMITATION OF ABSTRACT	18. NUMBER OF PAGES	19a. NAME OF RESPONSIBLE PERSON
a. REPORT **unclassified**	b. ABSTRACT **unclassified**	c. THIS PAGE **unclassified**	**Same as Report (SAR)**	**24**	

Standard Form 298 (Rev. 8-98)
Prescribed by ANSI Std Z39-18

Final Report for AOARD Grant FA2386-13-1-4035 "Development of single-molecule DNA sequencing platform based on single-molecule electrical conductance"

Date: May 25, 2015

PI information: G. Steven Huang; gstevehuang@mail.nctu.edu.tw, gstevehuang@gmail.com ; National Chiao Tung University; Department of Materials Science and Engineering; 1001 University Rd., Hsinchu, Taiwan, ROC; Phone: 886-939-919973; Fax: 886-3-5131451.

Period of Performance: March/20/2013 – March/19/2015

Abstract: We have demonstrated single-molecule sequencing based on the protein transistor. However, the utility relies on the stability of the molecular device. Thus this project has focused on the key issue of the molecular electronic device, effect of the bio-nano interface on the immune system.

The key component of the protein transistor is the binding interface of gold nanoparticles (GNPs) and antibody. To investigate the effect of GNPs on the immune system, B-cells were treated with GNPs with diameters ranging from 2 to 50 nm. The GNPs enhanced IgG secretion in a size-dependent manner, with a peak of efficacy at 10 nm. This enhancing effect was validated *ex vivo* using B-cells isolated from mouse spleen. GNP-treatment upregulated B-lymphocyte-induced maturation protein 1 (blimp1) and downregulated paired box 5 (pax5). Immunostaining for Blimp1 and Pax5 in B-cells confirmed that the GNPs stimulated IgG secretion through the blimp1/pax5 pathway. The immunization of mice using peptide-conjugated GNPs indicated that the GNPs were capable of enhancing humoral immunity in a size-dependent manner. This effect was consistent with the bio-distribution of the GNPs in mouse spleen. In conclusion, *in vitro*, *ex vivo*, and *in vivo* evidence supports our hypothesis that GNPs enhance humoral immunity in a size-dependent manor. In addition to their toxicity in human health and in environmental impact, the immune-stimulatory activity of nanoparticles could be applied to generate immunoglobulins with high specificity to GNPs, thus serve as the foundation for a stable molecular device.

Introduction: Years before the completion of Human Genome Project using first-generation Sanger sequencing, the next-generation sequencing technologies have been developed based on arrayed reactions that sequence amplified DNA targets. The third-generation sequencing method (single-molecule sequencing technology) was proposed without the need of amplification, ligation or cloning. Current technology suffers the short read-length and high error rate which limit further application to unknown genomes (*1-9*).

We proposed to develop a single-molecule sequencing technology based on the electrical conductance of single-molecule DNA polymerase. A protein transistor (proT), which provides stable conductance readings, was designed to hold DNA polymerase during the synthesis of a new

strand (*10*). ProT is a molecular device composed of immunoglobulin G (IgG) holding two gold nanoparticles (NP), which are separately attached to two electrodes. The IgG antibody binds to NPs through stable molecular junctions, leading to the stable and reproducible transfer characteristics of the device. As the electrical conductivity of DNA polymerase can be directly measured by conjugating the enzyme to a proT, the conductance trajectory may be useful in decoding a DNA sequence during nucleotide incorporation.

The key issue in this technology is the stability of the molecular device. The interaction between antibody and gold nanoparticles is the key to resolve this issue. We investigated the bio-nano interface through the immune response of gold nanoparticles. This is revealed by the study of "Gold nanoparticles regulate the blimp1/pax5 pathway and enhance antibody secretion in B-cells".

GNP conjugates have been used in biomedical diagnostics and analytics, photothermal and photodynamic therapies, and drug delivery (*11-13*), in particular, targeted drug delivery in antitumor treatment (*14*). Active targeting provides a powerful approach to increasing drug efficacy at specific sites. However, the potential toxicological and immunologic effects of nanoparticles may reduce drug efficacy in therapeutic treatment.

The *in vitro* and *in vivo* toxicity of GNPs has been investigated, mostly *in vitro*. GNPs enter cells in a size- and shape-dependent manner (*15, 16*). The uptake of GNPs reaches a maximum when the size nears 50 nm and when the aspect ratio approaches unity. The transport efficiency reaches a plateau 30 min after incubation. The uptake of GNPs is consistent with receptor-mediated endocytosis. Nevertheless, most GNPs can enter cells efficiently, and most studies indicate that they are nearly harmless to cultured cells (*17-20*). The bio-distribution of injected GNPs has shown a size-dependent accumulation in liver, spleen, and kidney (*21*). Although biocompatibility is associated with GNPs, the injection of GNPs causes impairment of cognition in mice (*22*). A heavy dose of GNPs has lethal size-dependent effects, most notably on the ability of modified GNPs to stimulate antibody secretion (*23, 24*). It should be noted that GNPs enhance a focused antigenic response, which corresponds to the accumulation of GNPs in the spleen.

GNPs interact substantially with the immune system. Colloidal gold is an extraordinary carrier that can be used to generate antibodies against relatively small haptens, such as glutamate (*25-27*). As a carrier, the immunogenic properties of gold nanoparticles have been reported (*28*). GNPs are toxic *in vivo* and have immunogenic properties that are associated with their lethal effects (*23*). GNPs also show size-dependent immune-stimulating activity when used as vaccine carriers (*24*). In a recent report, 10 nm GNPs induced the transcriptional activation of NF-kB in a B-lymphocyte cell line (*29*). Treatment with 10 nm GNPs induced the activation of an NF-kB-regulated reporter gene. An interaction with the cysteine residues on IkB kinases (IKK), NF-kB signal transduction proteins, was proposed as a mechanism. The activation of the canonical NF-kB signaling pathway is indicated by IkBa phosphorylation, followed by IkBa degradation and increased nuclear RelA localization. The expression of an IkBa suppressor

reversed GNP-induced NF-kB activation. This *in vitro* evidence clearly indicates that GNP-cell interactions can be specific, particularly in B-cells. We hypothesize that GNPs may affect the antibody secretion of B-cells through specific signal transduction pathways and in a size-dependent manner.

Experiment:

Preparation and characterization of gold nanoparticles

GNPs of 2, 5, 8, 12, 17, 37, and 50 nm in diameter were synthesized as reported previously (*24*). The seed colloids were prepared by adding 1 mL of 0.25 mM $HAuCl_4$ to 90 mL of H_2O and stirring for 1 min at 25 °C. Two milliliters of 38.8 mM sodium citrate was added to the solution and stirred for 1 min, followed by the addition of 0.6 mL freshly prepared 0.1 M $NaBH_4$ in 38.8 mM sodium citrate. The solution was stirred for an additional 5-10 min at 0-4 °C. Different diameters of GNPs, ranging from 2 to 50 nm, were generated by changing the volume of the seed colloid added. The reaction temperature and time were adjusted to control the size of the GNPs. All the synthesized GNPs were characterized by UV absorbance and verified by electron microscopy or atomic force microscopy.

Cell culture

Murine antibody-generating cells against haptoglobin (5B1B3 B cells, splenocytes fused with myeloma cells) were cultured in DMEM (GIBCO, Gaithersburg, MD) containing 10% fetal bovine serum (FBS) (Jacques Boy, Reims, France), 2 mM L-glutamine (Boehringer, M12-702, Mannheim, Germany), 100 U/mL penicillin (GIBCO) and 100 U/mL streptomycin (GIBCO) at 37 °C, 5% CO_2, and 99% humidity. Cells in the exponential growth phase at a minimum density of 1×10^6 cells/mL were collected and assayed for IgG secretion.

Designing of Synthetic peptide

The immunogenic peptides against the foot and mouth disease virus (FMDV) were designed and synthesized based on viral protein 1 of type O FMDV. The amino acid sequence for pFMDV is NGSSKYGDTSTNNVRGDLQVLAQKAERTLC. An extra cysteine was added to the C-terminus of each peptide to improve the binding to the gold surface (*30*). The conjugation of the antigen with the GNPs was performed by titrating the antigens into a GNP solution. The titration was monitored by UV absorption at the wavelength appropriate for each peptide to detect the aggregation of unsaturated GNP in the presence of 1 M sodium chloride. The conjugated complexes were purified by centrifugation and resuspended in PBS at a final concentration of 0.01 µg/µl.

Immunization of mice

The animal treatments were performed according to “The Guidelines for the Care and Use of

Experimental Animals" of National Chiao Tung University. Four-week-old male BALB/C mice were housed at 22±2 °C with a 12-h light/dark cycle and fed standard rodent chow and water ad libitum. The mice were randomly assigned to the experimental groups. Each group consisted of six mice.

The groups of 4-week-old BALB/c mice were given intraperitoneal (IP) and subcutaneous (SC) immunizations of GNPs (8 nm or 12 nm) conjugated with pFMDVA, pFMDVB, pFMDVC, pFMDVD, and pFMDV. Those antigens were mixed with equal volumes of complete and incomplete adjuvant before administration. For all groups, the mice were immunized on weeks 0, 1, 2, 3, 5, 7, and 9, and blood was collected from the tail vein after weeks 4, 6, 8, and 10. The sera were collected after centrifugation and stored at −20 ˚C. The animals were sacrificed at the end of the experiment by cardiac puncture under CO_2 anesthesia. The spleens were isolated, and the organ weights of all the mice were measured.

Inductively coupled plasma mass spectrometry (ICP-MS)

For the total element determinations, standard solutions were prepared by the dilution of a multi-element standard (1,000 mg L^{-1} in 1 M HNO_3) obtained from Merck (Darmstadt, Germany). Nitric acid (65%), hydrochloric acid (37%), perchloric acid (70%), and hydrogen peroxide (30%) of Suprapur® grade (Merck) were used to mineralize the samples. A size-exclusion column was connected to the ICP-MS apparatus. The spleen samples were homogenized in 25 mM Tris (hydroxymethyl) aminomethane (Tris)–12.5 mM HCl buffer solution at pH 8 and centrifuged at 13,000 rpm for 1 hour. The supernatant was applied to the size-exclusion column of the HPLC system, which had been equilibrated with 25 mM Tris–12.5 mM HCl (containing 20 mM KCl), and was eluted with the same buffer at a flow rate of 1 mL/min. The metal components of the metal-binding proteins that were eluted from the HPLC system were detected by ICP-MS (Perkin Elmer, SCIEX ELAN 5000). The main operating conditions were as follows: RF power, 1900 W; carrier gas flow, 0.8 L/min Ar; and makeup gas flow, 0.19 L/min Ar.

Enzyme-linked immunosorbent assay (ELISA)

Each well of an ELISA plate (Nunc, Roskilde, Denmark) was coated with haptoglobin (0.02 μg/μl) in phosphate buffered saline (PBS). The unbound proteins were washed 3 times with PBS followed by incubation with 1% (wt/vol) skim milk for 2 h at 37 ℃. One hundred microliters of culture medium (2-3 weeks following the fusion) was added and incubated at room temperature for 1 h. Each well was washed 3 times with PBS containing 0.05% Tween-20. The bound antibodies were detected using a goat anti-mouse IgG conjugated to horseradish peroxidase (HRP) at 37℃ for 1 h in PBS containing 0.05% Tween-20. Finally, each well was washed and developed with 3,3',5,5'-Tetramethylbenzidine (TMB), and the binding efficiency was monitored by measuring the absorbance at 405 nm.

Reverse Transcription polymerase chain reaction (RT-PCR)

Total RNA was extracted from 10^6 cells using TRI-reagent (Talron Biotech) according to the manufacturer's instructions. The RNA was isolated by chloroform extraction and isopropanol precipitation, followed by ethanol washes to remove the impurities and unwanted organic compounds. The purified RNA was resuspended in DEPC-treated water and quantified by measuring the OD260. The OD260-to-OD280 ratio usually exceeded 2.0. Following the spectrophotometric determination of the RNA yield, cDNA was synthesized with oligo(dT) primers by reverse transcription using SuperScript III Reverse Transcriptase (Invitrogen). An aliquot of the cDNA was subjected to 30 cycles of PCR using a standard procedure denaturing at 94 °C for 30 s, annealing the B-lymphocyte-induced maturation protein 1 (blimp1) and GAPDH primers at 55 °C, or the paired box 5 (pax5) primers at 45 °C for 30 s, and elongating at 72 °C for 1 min. The amplified products were resolved on a 1.8% agarose gel and visualized by ethidium bromide staining. The respective forward and reverse primers used for the amplifications were 5'-TGGACTGGGTGGACATGAGAG-3' and 5'-AAGTGGTGGA-ACTCCTCTCTG-3' for *blimp1*; 5'-TTATGAGACAGGAAGCATCAAGC-3' and 5'-CGTGTTTGAGAGACAGCACTAC-3' for *pax5*; and *5'*-GCCTACCTCATGGGACTGAA-3' and 5'-ACATTCTGCCCTTTGGTGAC-3' for *GAPDH*.

Western blot analysis

SDS-PAGE using 15% polyacrylamide gels (unless specified otherwise) was used to analyze the cell lysate using a modified procedure described previously (*31*). Electrophoresis was conducted in a vertical slab gel unit (Mini PIII, Bio-Rad, Hercules, CA) equipped with a PAC 300 power supply (Bio-Rad). All of the SDS-PAGE samples (20 μg) were equilibrated in 10 mM Tris-HCl and 5% SDS (pH 7.6) before being loaded onto the gel. Following electrophoresis, the gel was soaked briefly and rapidly in a transfer buffer containing 25 mM Tris, 192 mM glycine, 20% methanol, and 0.0375% SDS (pH 8.3) for 30 s. The gel was then immediately electrotransferred to a PVDF membrane at 90 mA for 60 min in a semi-dry transfer apparatus (Bio-Rad). The membrane was immersed in 5% skim milk for 1 h with gentle shaking. Following three washes with PBS for 5 min each, the membrane was incubated for 1 h at room temperature with a mouse monoclonal antibody raised against Blimp1 (Abcam) and Pax 5 (Cell Signaling) at 1:1000 dilutions in PBS containing 0.1% skim milk and 0.05% (v/v) Tween-20. The membrane was washed three times with the same dilution buffer and was then incubated with a commercially available goat anti-mouse IgG conjugated with horseradish peroxidase (Chemcon; Temecula, CA) at a 1:10,000 dilution for 1 h. Finally, the membrane was developed using chemiluminescence. The chemiluminescent detection was performed using western blotting luminol and oxidizing reagents (U.S.A.).

Immunofluorescent staining

Glass cover slips were sterilized by immersing them in 75% ethanol, drying them over a flame, and placing them into the wells of a 6-well culture plate. The hybridoma cells (5×10^6) in 2 mL of DMEM medium containing 10% FBS were seeded over the individual cover slips and grown at 37 °C to 50-70% confluence. Following the removal of the culture medium, the cells in each well were rinsed twice with PBS and fixed with 4% paraformaldehyde (Sigma) in PBS and then incubated at room temperature for 15 min. After three rinses with PBS, the cells were treated with 0.1% Triton X-100 (pH 8.0) at room temperature for 15 min. Following the washes with PBS, the cover slips were incubated in 1% bovine serum albumin (BSA) to block nonspecific staining and were then incubated with a primary mouse antibody against anti-Blimp1 (diluted 1:400) and a rabbit antibody against anti-Pax5 (diluted 1:50) at 4℃ overnight. After PBS washes, the cells were incubated with Alexa Fluor 488 goat anti-mouse antibody, Dylight™ 549-conjugated AffiniPure goat anti-rabbit antibody and DAPI for 1.5 h. The samples were mounted and imaged using a Leica TCS SP2 confocal microscope.

Statistical Analyses

All data are presented as the means ± standard deviation (SD), with a minimum of six mice in each group. The concentrations of biogenic amines and Ach in the spleen samples were analyzed using an unpaired Student's *t*-test. The criterion for statistical significance was $p < 0.05$ for all statistical evaluations.

Results and Discussion:

GNPs enhanced immunoglobulin G (IgG) secretion in B-cells

To investigate the immune-stimulating activity of the GNPs, 5B1B3 mouse hybridoma cells (secreting anti-haptoglobin IgG) were treated with GNPs ranging from 2 to 50 nm for 6, 12, 18 and 24 hours (figure 1). The secretion of IgG into the culture media was quantified by ELISA. The GNPs enhanced IgG secretion by the 5B1B3 cells. The IgG secretion peaked at 12 to 18 hrs after the treatment and returned to baseline at 24 hrs. The enhancing effect was size-dependent. The maximum stimulation occurred between 2 and 12 nm. The cell viability did not vary significantly with GNP treatment, indicating that the stimulation of IgG secretion was not dependent on cell number. To verify the antibody-stimulatory activity of the GNPs, B-cells were isolated from mouse spleens and treated with GNPs (figure 2). The GNP treatment enhanced IgG secretion at 12 and 18 hr. The enhancing effect was at a maximum for the 8-nm and 12-nm GNPs. The enhancing effect of the GNPs on the B-cells was analogous to that for the hybridoma cells. The *in vitro* and *ex vivo* evidence indicates that the GNPs stimulated humoral immunity in a size-dependent and time-dependent manner.

GNPs regulated blimp1/pax5 pathway

B-lymphocyte-induced maturation protein 1 (blimp1) and paired box 5 (pax5) are key factors that

regulate the secretion of IgG in B-cells (*22, 23*). The expression of blimp1 positively regulates the secretion of IgG, while pax5 down regulates IgG secretion. To test the hypothesis that GNPs may enhance IgG secretion via the blimp1/pax5 pathway, RT-PCR and Western blot were performed (figure 3, 4). In general, the levels of transcription and protein expression for blimp1 and pax5 were complementary. The expression of blimp1 increased in B-cells during both the 12-hr and 18-hr treatments with 2 to 12 nm GNPs. The levels of pax5 expression decreased under the same conditions. The results suggest that the GNPs stimulated IgG secretion by B-cells through the blimp1/pax5 pathway.

To verify the cellular localization of Blimp1 and Pax5 when stimulated by GNPs, immunofluorescent staining for both Blimp1 and Pax5 was performed and images were generated using confocal microscopy (figure 5). Blimp1 was expressed and localized near the cell membrane of the GNP-activated B-cells, while Pax5 was found in quiescent B-cells. The temporal and size-dependent activation of the blimp1/pax5 pathways was therefore validated using this immunofluorescence staining technique.

GNP injection enhanced humoral immunity in mice

The GNPs enhanced IgG secretion in both the hybridomas and B-cells. The *in vivo* stimulatory activity of the GNPs remains to be explored. To evaluate humoral immunity, mice were immunized with peptide-conjugated GNPs. The peptides were synthesized based on the amino acid sequence of the VP1 coat protein of the FMDV (table 1). The peptide pFMDVD (19 amino acids in length) and pFMDV (24 a.a. in length) were both conjugated to GNPs ranging from 2 to 50 nm and injected into mice. The serum titer was verified at the end of the fourth week (figure 6). The longer peptide induced a higher titer than the shorter peptide. Under both conditions, the GNPs ranging from 2 to 17 nm induced higher antibody titers. We have previously shown that the size-dependent immune-stimulatory activity of the GNPs is associated with the presence of GNPs in the spleen (*23*). To verify that the presence of GNPs in spleen is affected by the length of the conjugated peptide, five peptides of different lengths (pFMDVA, pFMDVB, pFMDVC, pFMDVD, and pFMDVE; table 1) were conjugated to 8 nm and 12 nm GNPs and injected into mice. The 12 nm GNPs showed higher levels of accumulation in the spleen than the 8 nm GNPs (figure 5). Within the same group, all lengths of the peptide showed similar levels of accumulation, including the unmodified GNPs. In summary, the accumulation of GNPs in the spleen is less associated with the immune-stimulatory ability of GNPs. The accumulation of GNPs in the spleen is size-dependent but is less dependent on the length of the peptides conjugated to the GNPs.

Nanoparticle-based delivery systems are expected to be advantageous for site-specific delivery, improved *in vitro* and *in vivo* stability, and reduced side effect profile. The primary function of the immune system is to protect the host from foreign substances; however, the recognition of

nanoparticles as foreign by the immune cells may result in a multilevel immune response against the nanoparticles and may eventually lead to toxicity in the host and/or lack of therapeutic efficacy due to the scavenging activity of the immune system. Previous studies have indicated that nanoparticles are often scavenged by the phagocytic cells of the immune system, i.e., macrophages (*23*). Furthermore, the enhancement of humoral immunity and the generation of antibodies specific to the surface antigens of particles may reduce the efficacy and the safety of nanoparticle-based therapeutics. The current study provides evidence for the size-dependent stimulation of humoral immunity. For the design of nanoparticles as drug carriers, diameters ranging from 2 to 12 nm should be avoided to minimize the immune-stimulatory effect.

We have previously shown that GNPs work as vaccine carriers when they stimulate a focused immune response (*24*). The current study provides further evidence that the enhancement of humoral immunity is size-dependent, time-dependent, and associated with the bio-distribution of GNPs.

The accumulation of GNPs in the spleen depends on the diameter of the GNPs (*14*). Surface modification of the length of the peptide did not significantly alter the biodistribution of GMPs in the spleen. The GNPs enter cells in a size- and shape-dependent manner mediated by a membrane receptor (*15, 16, 31-33*). The uptake of GNPs reaches a maximum when the size nears 50 nm and when the aspect ratio approaches unity (*32*). GNPs of diameters ranging from 2 to 100 nm alter the signaling processes essential for basic cell functions, including cell death (*34*). The current study explored the regulation of signal transduction pathways in B-cells. Blimp1 is a transcriptional repressor that acts as an essential transcriptional activator for high-level immunoglobulin synthesis (*35, 36*). Additionally, blimp 1 represses pax5, which relieves the repression on the immunoglobulin genes, allowing their upregulation (*37*). Blimp1 and Pax5 regulate the differentiation of mature B cells into antibody-secreting plasma cells (*37, 38*).

The enhancement of antibody secretion in B-cells by GNPs likely occurs through the blimp1/pax5 signal transduction pathways. The upregulation of blimp1 and downregulation of pax5 is closely associated with the size and time of treatment with GNPs. This result is consistent with previous findings that GNPs upregulate NF-kB in mouse B-cells (*29*). However, we cannot exclude the possibility that cell death might contribute to this enhancement. Figure 1B shows an increase in cell viability upon GNP treatment. The tendency towards viability is consistent with antibody secretion. The lack of significance in the viability statistics might be due to insufficient numbers of repeats performed in the current study. However, the effect of GNP-induced cell-death suppression on the enhancement of antibody secretion could work as an alternative pathway in parallel to the blimp1/pax5 pathways.

Conclusions

In conclusion, the *in vitro*, *ex vivo*, and *in vivo* evidence suggests that GNPs activate B-cells and enhance immunoglobulin G secretion. GNP treatment upregulates blimp1, downregulates pax5,

and enhances downstream IgG secretion. The enhancement is size dependent and time dependent. GNPs ranging from 2 to 12 nm had the maximum stimulatory activity for the production of antibody.

Significance and perspectives

This is the first time that specific signal transduction pathway has been unambiguously identified and assigned to nanoparticles in a size-dependent manner. We have thus established the link between physical dimension and biological response at molecular level. In the future, it is possible to imitate this physical stimulation through "non-physical" manipulation, such as genetic control. In particular, the interaction of immune system and nanoparticles could be manipulated through genetic control. The instant advantage is to establish stable and high affinity bionano interface in the fabrication of the unique molecular electronic device, the protein transistor.

References

1. Bentley, D. R. (2006) Whole-genome re-sequencing, *Curr. Opin. Genet. Dev. 16*, 545-552.
2. Schadt, E. E., Turner, S., and Kasarskis, A. (2010) A window into third-generation sequencing, *Human Molecular Genetics 19*, R227-R240.
3. Cherf, G. M., Lieberman, K. R., Rashid, H., Lam, C. E., Karplus, K., and Akeson, M. (2012) Automated forward and reverse ratcheting of DNA in a nanopore at 5-A precision, *Nat Biotech 30*, 344-348.
4. Schneider, G. F., and Dekker, C. (2012) DNA sequencing with nanopores, *Nat Biotech 30*, 326-328.
5. Shendure, J., and Ji, H. (2008) Next-generation DNA sequencing, *Nat Biotech 26*, 1135-1145.
6. Pushkarev, D., Neff, N. F., and Quake, S. R. (2009) Single-molecule sequencing of an individual human genome, *Nature Biotechnology 27*, 847-U101.
7.Choi, Y., Moody, I. S., Sims, P. C., Hunt, S. R., Corso, B. L., Perez, I., Weiss, G. A., and Collins, P. G. (2012) Single-Molecule Lysozyme Dynamics Monitored by an Electronic Circuit, *Science 335*, 319-324.
8. Harris, T. D. (2008) Single-molecule DNA sequencing of a viral genome, *Science 320*, 106-109.
9. Gupta, P. K. (2008) Single-molecule DNA sequencing technologies for future genomics research, *Trends in Biotechnology 26*, 602-611.
10. Chen, Y.-S., Hong, M.-Y., and Huang, G. S. (2012) A protein transistor made of an antibody molecule and two gold nanoparticles, *Nature Nanotechnology 7*, 197-203.
11. Dreaden, E. C., Alkilany, A. M., Huang, X. H., Murphy, C. J., and El-Sayed, M. A. (2012) The golden age: gold nanoparticles for biomedicine, *Chem. Soc. Rev. 41*, 2740-2779.
12. Dykman, L., and Khlebtsov, N. (2012) Gold nanoparticles in biomedical applications: recent advances and perspectives, *Chem. Soc. Rev. 41*, 2256-2282.

13. Sardar, R., Funston, A. M., Mulvaney, P., and Murray, R. W. (2009) Gold Nanoparticles: Past, Present, and Future, *Langmuir 25*, 13840-13851.
14. Llevot, A., and Astruc, D. (2012) Applications of vectorized gold nanoparticles to the diagnosis and therapy of cancer, *Chem. Soc. Rev. 41*, 242-257.
15. Chithrani, B. D., and Chan, W. C. W. (2007) Elucidating the mechanism of cellular uptake and removal of protein-coated gold nanoparticles of different sizes and shapes, *Nano Letters 7*, 1542-1550.
16. Chithrani, B. D., Ghazani, A. A., and Chan, W. C. W. (2006) Determining the size and shape dependence of gold nanoparticle uptake into mammalian cells, *Nano Letters 6*, 662-668.
17. Becker, M. L., Bailey, L. O., and Wooley, K. L. (2004) Peptide-derivatized shell-cross-linked nanoparticles. 2. Biocompatibility evaluation, *Bioconjugate Chemistry 15*, 710-717.
18. Connor, E. E., Mwamuka, J., Gole, A., Murphy, C. J., and Wyatt, M. D. (2005) Gold nanoparticles are taken up by human cells but do not cause acute cytotoxicity, *Small 1*, 325-327.
19. Hauck, T. S., Ghazani, A. A., and Chan, W. C. W. (2008) Assessing the effect of surface chemistry on gold nanorod uptake, toxicity, and gene expression in mammalian cells, *Small 4*, 153-159.
20. Paciotti, G. F., Myer, L., Weinreich, D., Goia, D., Pavel, N., McLaughlin, R. E., and Tamarkin, L. (2004) Colloidal gold: A novel nanoparticle vector for tumor directed drug delivery, *Drug Delivery 11*, 169-183.
21. Sonavane, G., Tomoda, K., and Makino, K. (2008) Biodistribution of colloidal gold nanoparticles after intravenous administration: Effect of particle size, *Colloids and Surfaces B-Biointerfaces 66*, 274-280.
22. Chen, Y.-S., Hung, Y.-C., Lin, W.-H., and Huang, G. S. (2010) Assessment of gold nanoparticles as a size-dependent vaccine carrier for enhancing the antibody response against synthetic foot-and-mouth disease virus peptide, *Nanotechnology 21*.
23. Chen, Y.-S., Hung, Y.-C., Liau, I., and Huang, G. S. (2009) Assessment of the In Vivo Toxicity of Gold Nanoparticles, *Nanoscale Research Letters 4*, 858-864.
24. Chen, Y.-S., Hung, Y.-C., Lin, L.-W., Liau, I., Hong, M.-Y., and **Huang*, G. S.** (2010) Size-dependent impairment of cognition in mice caused by the injection of gold nanoparticles, *Nanotechnology 21*, 485102.
25. Dykman, L. A., Matora, L. Y., and Bogatyrev, V. A. (1996) Use of colloidal gold to obtain antibiotin antibodies, *J. Microbiol. Methods 24*, 247-248.
26. Ottersen, O. P., and Stormmathisen, J. (1987) LOCALIZATION OF AMINO-ACID NEUROTRANSMITTERS BY IMMUNOCYTOCHEMISTRY, *Trends Neurosci. 10*, 250-255.
27. Shiosaka, S., Kiyama, H., Wanaka, A., and Tohyama, M. (1986) A NEW METHOD FOR PRODUCING A SPECIFIC AND HIGH TITER ANTIBODY AGAINST GLUTAMATE USING COLLOIDAL GOLD AS A CARRIER, *Brain Res. 382*, 399-403.

28. Dykman, L. A., Sumaroka, M. V., Staroverov, S. A., Zaitseva, I. S., and Bogatyrev, V. A. (2004) Immunogenic properties of colloidal gold, *Biol. Bull 31*, 75-79.
29. Sharma, M., Salisbury, R. L., Maurer, E. I., Hussain, S. M., and Sulentic, C. E. W. (2013) Gold nanoparticles induce transcriptional activity of NF-kappa B in a B-lymphocyte cell line, *Nanoscale 5*, 3747-3756.
30. Slot, J. W., and Geuze, H. J. (1985) A new method of preparing gold probes for multiple-labeling cytochemistry, *Eur J Cell Biol 38*, 87-93.
31. Chen, W. L., Liu, W. T., Yang, M. C., Hwang, M. T., Tsao, J. H., and Mao, S. J. (2006) A novel conformation-dependent monoclonal antibody specific to the native structure of beta-lactoglobulin and its application, *J Dairy Sci 89*, 912-921.
32. Shukla, R., Bansal, V., Chaudhary, M., Basu, A., Bhonde, R. R., and Sastry, M. (2005) Biocompatibility of gold nanoparticles and their endocytotic fate inside the cellular compartment: a microscopic overview, *Langmuir 21*, 10644-10654.
33. Wang, S. H., Lee, C. W., Chiou, A., and Wei, P. K. (2010) Size-dependent endocytosis of gold nanoparticles studied by three-dimensional mapping of plasmonic scattering images, *Journal of Nanobiotechnology 8*, 33.
34. Jiang, W., Kim, B. Y. S., Rutka, J. T., and Chan, W. C. W. (2008) Nanoparticle-mediated cellular response is size-dependent, *Nature Nanotechnology 3*, 145-150.
35. Klein, U., and Dalla-Favera, R. (2008) Germinal centres: role in B-cell physiology and malignancy, *Nature Reviews Immunology 8*, 22-33.
36. Nutt, S. L., Fairfax, K. A., and Kallies, A. (2007) BLIMP1 guides the fate of effector B and T cells, *Nature Reviews Immunology 7*, 923-927.
37. Lin, K. I., Angelin-Duclos, C., Kuo, T. C., and Calame, K. (2002) Blimp-1-dependent repression of Pax-5 is required for differentiation of B cells to immunoglobulin M-secreting plasma cells, *Molecular and cellular biology 22*, 4771-4780.
38. Savitsky, D., and Calame, K. (2006) B-1 B lymphocytes require Blimp-1 for immunoglobulin secretion, *The Journal of experimental medicine 203*, 2305-2314.

Table 1. Amino acid sequences of the synthetic peptides used to modify GNPs.

Synthesis peptide	Sequence
pFMDVA	ERTL(C)
pFMDVB	LAQKAERTL(C)
pFMDVC	GDLQVLAQKAERTL(C)
pFMDVD	TNNVRGDLQVLAQKAERTL(C)
pFMDV	YGDTSTNNVRGDLQVLAQKAERTL(C)

Figure 1. Effects of GNP treatment on the antibody secretion and cell viability of an IgG-secreting cell line. The antibody-generating cell line was treated with 5 μM GNPs, of diameters ranging from 2 nm to 50 nm, and incubated for 6, 12, 18 and 24 h. LPS served as a positive control. Medium and GNP supernatant served as negative controls. (a) Secreted antibody versus incubation time. (b) Cell viability versus incubation time. The amount of immunoglobulin G secretion was determined by ELISA. The results are expressed as the means ± SD (n=6). * $p<0.05$, ** $p<0.01$, *** $p<0.001$ when compared with medium control.

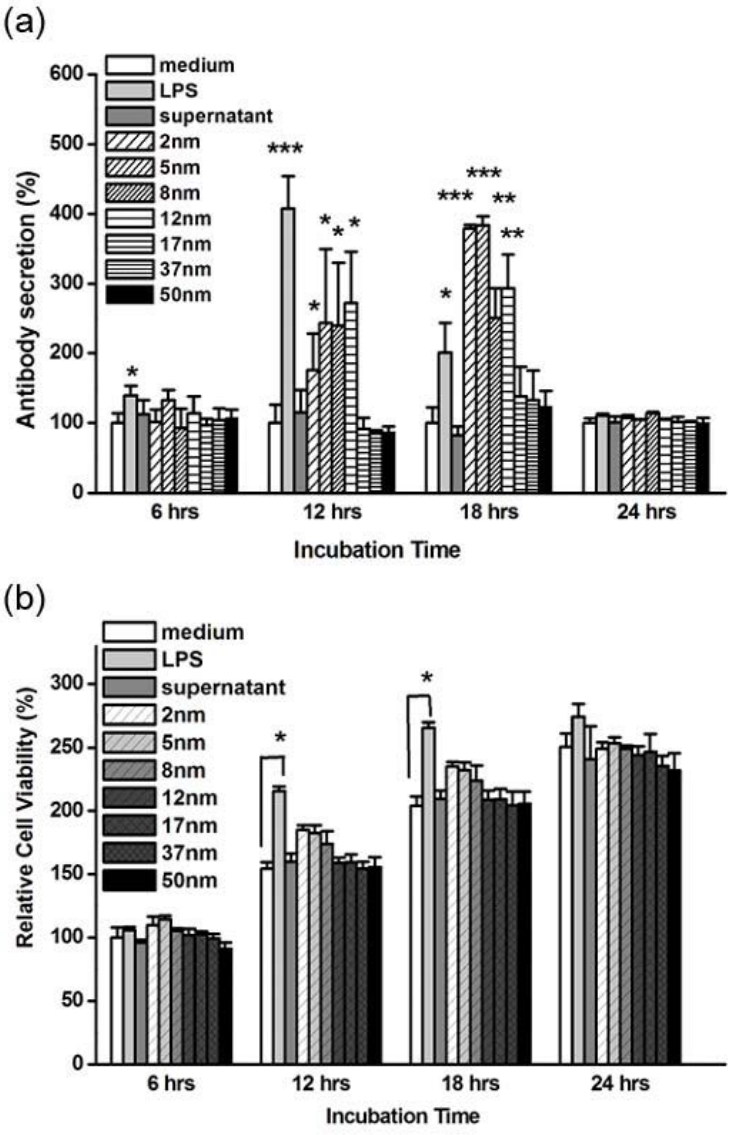

Figure 2. Effects of GNP treatment on the antibody secretion of B-cells isolated from splenocytes. B-cells were treated with 5 μM GNPs of diameters ranging from 2 nm to 50 nm and incubated for 6, 12, 18 and 24 h. LPS served as positive control. Medium and GNP supernatant served as negative controls. The amount of immunoglobulin G secretion was determined by ELISA. The results are expressed as the means ± SD (n=6). * $p<0.05$, ** $p<0.01$, *** $p<0.001$ when compared with medium control.

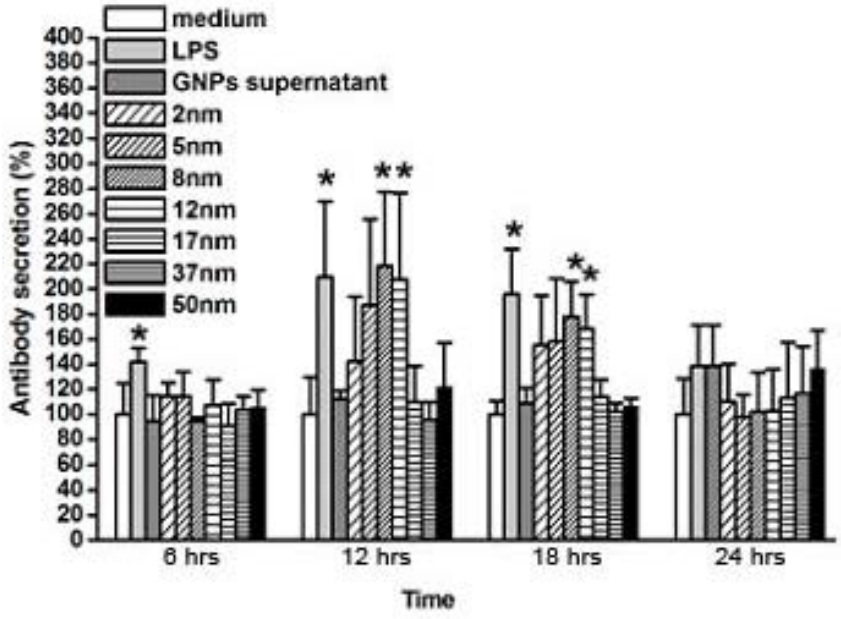

Figure 3. Effect of GNP treatment on the transcription levels of blimp1 and pax5 in antibody-secreting cells. The antibody-generating cells were treated with 5 μM GNPs for 6 h (a), 12 h (b), 18 h (c) and 24 h (d). The level of blimp1 and pax5 mRNA expression was determined by RT-PCR analysis and visualized by ethidium bromide staining of a 1.8% agarose gel. GAPDH was used as an internal control.

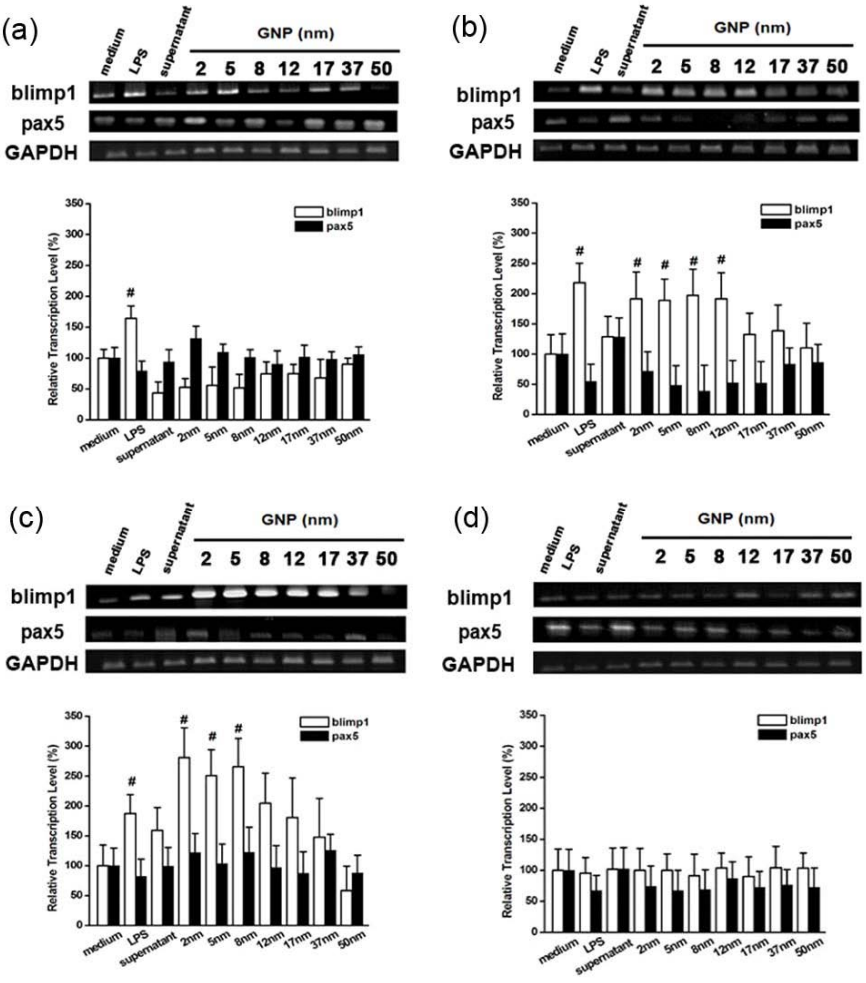

Figure 4. Western blot analysis of blimp1 and pax5 for antibody-generating cells treated with GNPs. The antibody-generating cells were treated with 5 μM GNPs for 6 h (a), 12 h (b), 18 h (c) and 24 h (d). Cell extracts were prepared and separated by 10% SDS-PAGE. Western blotting was performed using antibodies recognizing blimp1, pax5 and GAPDH. The measured specific bands were normalized against GAPDH. * P<0.05, ** P<0.01, *** P<0.001

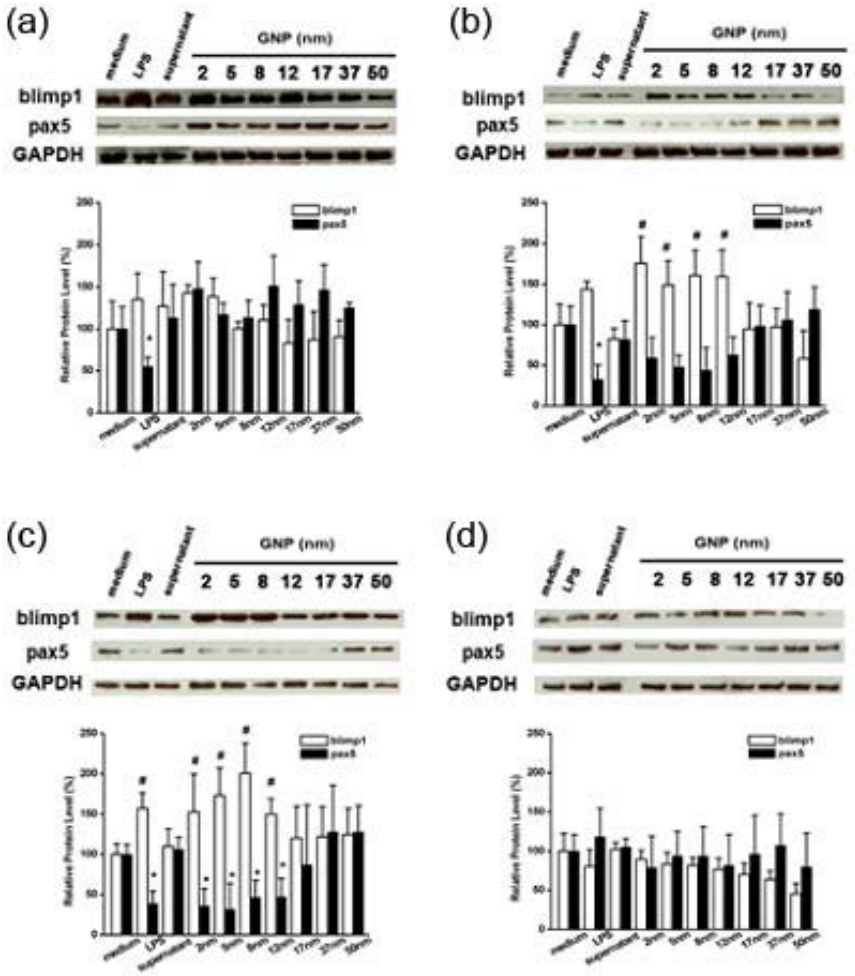

Figure 5. Immunostaining for blimp1 and pax5 in GNP-treated cells. (a) the antibody-generating cells were treated with GNPs for 12 h and 18 h, followed by immunostaining for blimp1 (green) and pax5 (red), which were visualized by confocal microscopy. DAPI staining was performed to localize the nuclei (blue). (b) Detailed images of cells treated with medium, LPS and 8 nm GNP for 12 hours.

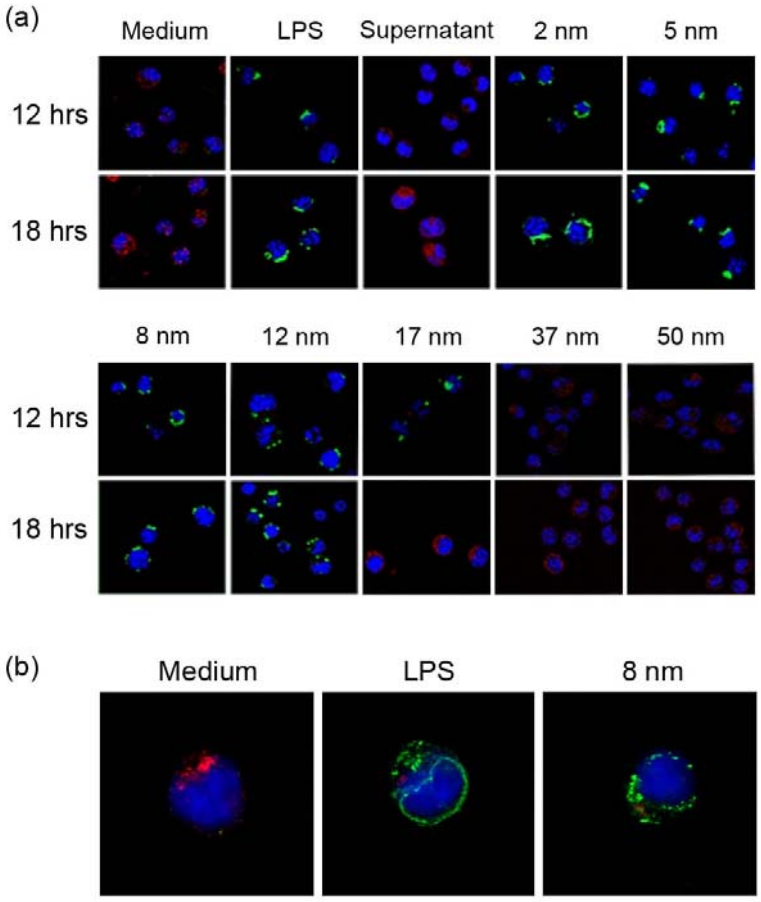

Figure 6. Titers of antisera from mice immunized with peptide-conjugated GNPs. (a) pFMDV-D (b) pFMDV carrying the amino acid sequence derived from FMDV (Table 1). The peptides were conjugated to KLH and served as control.

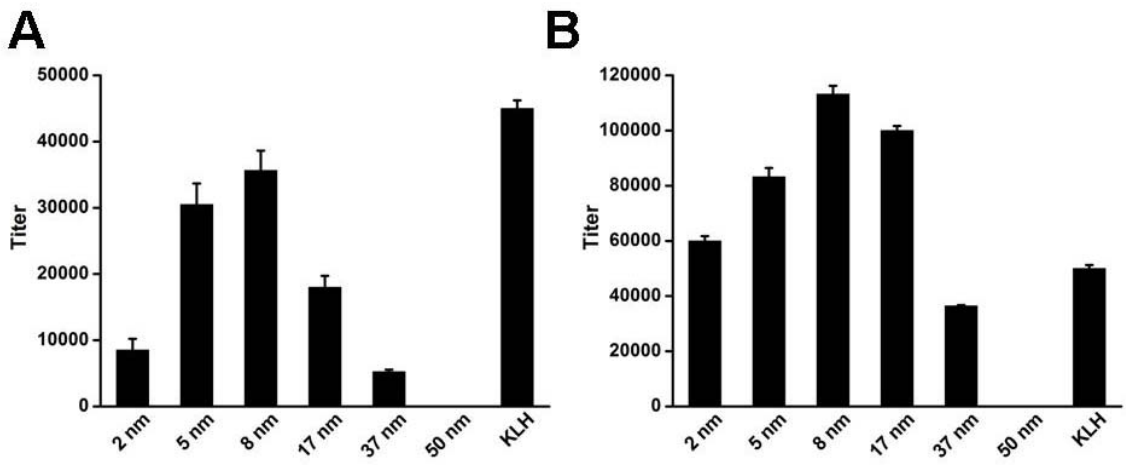

Figure 7. Biodistribution of the peptide-modified GNPs in mouse spleen. The mice were immunized with peptide-conjugated GNPs. The amounts of GNPs in the spleen were quantified by ICP-MS. Unmodified GNPs served as a negative control. The values shown are the means ± SD, averaged from six mice. (a) 8 nm GNP. (b) 12 nm GNP. Electron micrographs of the spleens from mice injected with (c) peptide-conjugated 8 nm GNP, and (d) peptide-conjugated 12 nm GNP. The scale bars represent 20 nm.

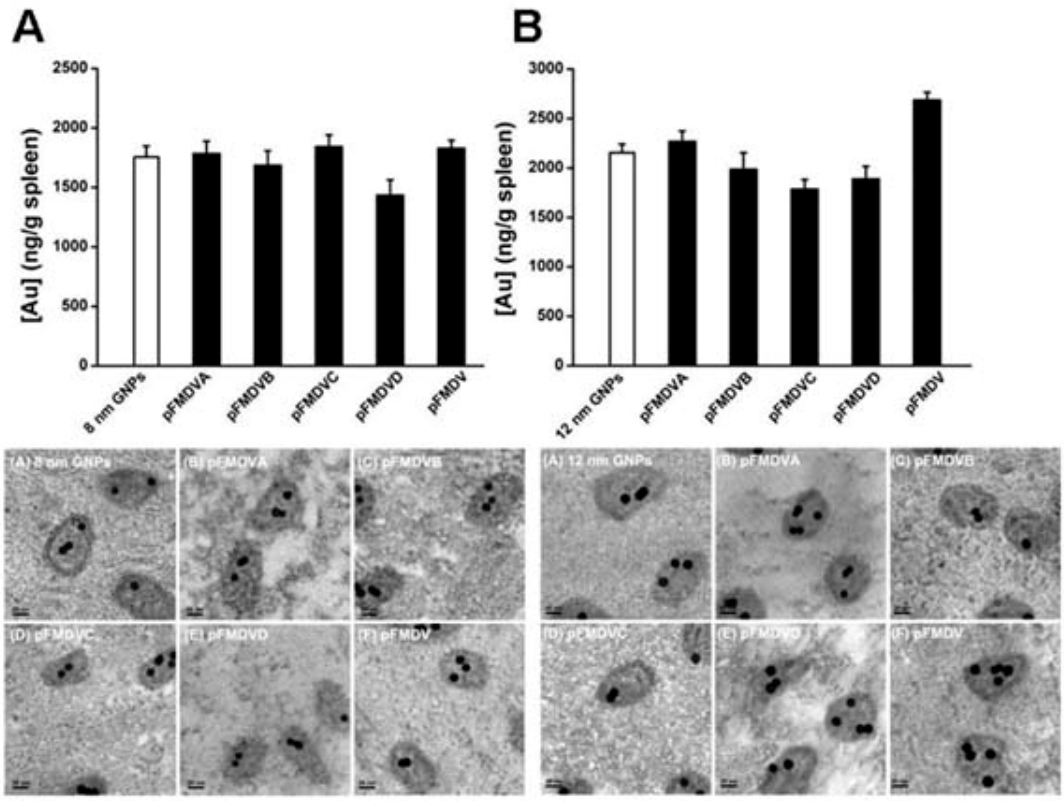

List of Publications and Significant Collaborations that resulted from your AOARD supported project: In standard format showing authors, title, journal, issue, pages, and date, for each category list the following:

a) papers published in peer-reviewed journals,

Chia-Hui Lee, Shih-Han Syu, Yu-Shiun Chen, Saber M Hussain,Andrei Aleksandrovich Onischuk, Wen Liang Chen, G. Steven Huang, Gold nanoparticles regulate the blimp1/pax5 pathway and enhance antibody secretion in B-cells, **Nanotechnology**, 25(12):125103, 2014

Chia-Hui Lee, Ya-Wen Cheng, G Steven Huang, Topographical control of cell-cell interaction in C6 glioma by nanodot arrays, **Nanoscale Research Letters**, 9(1):250, 2014

b) papers published in non-peer-reviewed journals or in conference proceedings,

c) conference presentations,

Yu-Shiun Chen, Bo-Hsiun Chen, Meng-Yen Hung, and G. Steven Huang, Single-molecule detection of spontaneous native protein ligation, BioBricks Foundation SB6.0, **The 6th International Meeting on Synthetic Biology**, Jul 9-11, 2013, Imperial College, London, UK

Yu-Shiun Chen, Chia-Hui Lee, Hsu-An Pan, Jin-Chern Chiou, Meng-Yen Hong and G. Steven Huang, DNA sequencing with electrical conductance measurements of a DNA polymerase, **2013 Biomedical Research Symposium of National Health Research Institutes**, Aug. 12-13

Wen-Liang Chen, Yu-Shiun Chen, Chia-Hui Lee, Shih-Han Syu, G. Steven Huang , Size-dependent control of humoral immunity in mice through blimp1/pax5 pathway by gold nanoparticles, **The Second International Conference on Life Science & Biological Engineering**, 7-9 November 2013, Osaka, Japan

G. Steven Huang, Yu-Shiun Chen, Chia-Hui Lee, Meng-Yen Hong , Folding and unfolding for an immunoglobulin G are structurally and energetically distinct, **2014 Gordon Research Conference,** Protein Folding Dynamics, 5-10 Jan, 2014, Hotel Galvez in Galveston TX, United States

Guewha Steven Huang , Single-Molecule Kinetics of DNA Polymerase, **2014 Biomedical Research Symposium of National Health Research Institutes and Dr. Monto Ho Memorial Symposium**

Chia-Hui Lee, Chun-Chung Huang, Guewha Steven Huang , Nano-Topographic and Temporal Control of NO Production in Cardiomyocytes, **Annual Conference on Engineering and Technology**, 16-18 October, 2014, Osaka, Japan

d) manuscripts submitted but not yet published, and

e) provide a list any interactions with industry or with Air Force Research Laboratory scientists or significant collaborations that resulted from this work.

1. **Saber M Hussain, co-author in the publication.**

2. **10th US Air Force - Taiwan Nanoscience Workshop** and Program Review, 20 – 22 Aug 2013, New Sanno Hotel, Tokyo, Japan, Title: Molecular electronics for single-molecule DNA sequencing

3. December 6, 2013, **onsite visit to NCTU** by AFOSR and officials from USA.

Institute	Position	Name
AR&L	Basic Research Directorate Fellow	Mahlet Mesfin
DASA (DE&C)	Deput for Country Program	David Macke
	Taiwan Desk Officer, ACD	Brain Edwards
LTC-Pacific, RDECOM	Director	Ken Evenson
	Specialist	Tommy Wong
NIPO	IEP&CWP Manager	Michael Locke
	Mine Warfare TPO	Ken Haas
Taiwan IEA NAVSEA HQ	Mine Warfare TPO	Steven Stumpp
Office of Naval Research	Office of Naval Research-Global Acting Director	Woei-Min Lin
Naval Medical Research Center-Asia	Captain Commanding Officer	Carlos Lebron

Institute	Position	Name
Office of Deputy Under Secretary of the Air Force/IA	Chief, ACD	David Rye
	International Agreement Specialist	Wasley Martin
Asian Office of Aerospace R&D	International Program Manager	LTC. Jermont Chen
PACAF Surgeon General's Office	Cooperative Health Engagement Staff	LTC. Wes Palmer

DD882: As a separate document, please complete and sign the inventions disclosure form.

Important Note: If the work has been adequately described in refereed publications, submit an abstract as described above but cite important findings to your above List of Publications, and if possible, attach any reprint(s) as an appendix. If a full report needs to be written, then submission of a final report that is very similar to a full length journal article will be sufficient in most cases.

This document may be as long or as short as needed to give a fair account of the work performed during the period of performance. There will be variations depending on the scope of the work. As such, there is no length or formatting constraints for the final report. Keep in mind the amount of funding you received relative to the amount of effort you put into the report. For example, do not submit a $300k report for $50k worth of funding; likewise, do not submit a $50k report for $300k worth of funding. Include as many charts and figures as required to explain the work.